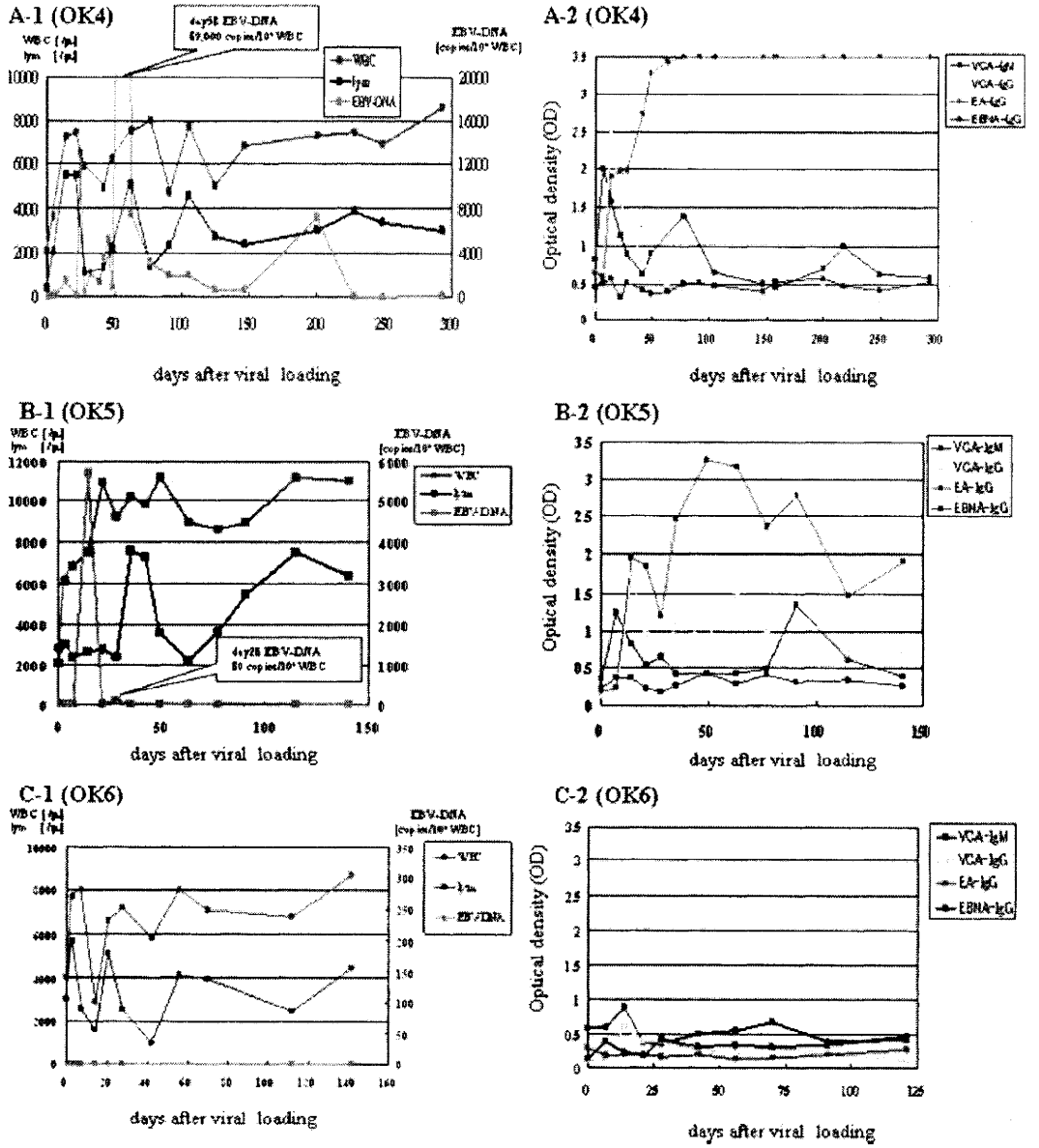

Fig. 1. Time course data of the peripheral blood tests in rabbits after intranasal or peroral inoculation of EBV. The numbers of white blood cells (WBCs), lymphocytes (lym), and EBV-DNA copy (A-1, B-1, and C-1) and the EBV-related antibody levels (A-2, B-2, and C-2) are indicated with the time course after EBV inoculation. When the EBV-DNA copy number was lower than the minimal sensitivity (20 copies/10^6 WBCs), it has been indicated as "0." OK4 (A-1,A-2) and OK5 (B-1,B-2) are EBV-DNA-positive rabbits. The data of OK6 (C-1,C-2) is shown as a representative EBV-DNA-negative rabbit. EBV-DNA was detected for more than 200 days in OK4 (from day 5: 1.0×10^2 copies/10^6 WBCs to day 249: 2.3×10^1 copies/10^6 WBCs, maximum: 8.9×10^4/10^6 WBCs on day 58), whereas, in OK5, EBV-DNA was detected transiently, that is, 5.7×10^3 copies/10^6 WBCs on day 14 and 8.0×10^2 copies/10^6 WBCs on day 28. The numbers of WBCs and lymphocytes tended to be elevated following EBV inoculation, but they were within normal limits in all rabbits. When the absorbance value of the EBV antibodies in plasma was higher than the maximal detection limit (more than 3.5) by ELISA, it is indicated as "3.5." The antibodies data of OK4, OK5, and OK6 are shown in A-2, B-2, and C-2, respectively. The high levels of EA-IgG were maintained during the observation period after a rapid EA-IgG increase in the early phase in all EBV-DNA-positive rabbits, although the EA-IgG value of OK4 was relatively higher than that in the other rabbits with transient EBV-DNA. The levels of both VCA-IgM and VCA-IgG were transiently increased in all the EBV-DNA-positive rabbits. The levels of EBNA-IgG were not increased even in EBV-DNA-positive rabbits. None of these antibody levels were increased in EBV-DNA-negative rabbits.

which was infected for a prolonged period, EBNA1 and EBNA2 expression and BZLF1 expression was detected intermittently from days 14 to 158 and from days 7 to 249, respectively, although *EA* was not detected. In OK5, the mRNAs of EA and EBNA2 were detected only on day 14, and that of BZLF1 was detected on days 14 and 21. In both OK8 and OK10, only BZLF1 was expressed on day 14 (data of OK10 are not shown). Expression of any of these genes was not detected in EBV-DNA-negative OK6, OK7, and OK9 during the experiment.

TABLE II. Summary of EBV-Inoculated Rabbits Used in This Study

Rabbit name	Inoculation route	Inoculated viral loads (copies)	Increase of anti-EBV antibody titer	EBV detection in PBMCs after viral inoculation			ISH, EBER1	Immunohistochemistry			
				EBV-DNA (copies/10^6 WBC)	EBV-mRNA (RT-PCR)	Observation period (outcome)		EBNA2	LMP1	ZEBRA	EA
OK4[a]	IN and PO	1.5×10^9	+ (EA-IgG, VCA-IgM, and VCA-IgG)	Continuously + 8.9×10^4 (day 63)	− (EBNA1, EBNA2, BZLF1)	396 days (alive)	ND	ND	ND	ND	ND
OK5[b]	IN	1.7×10^9	+ (EA-IgG, VCA-IgM, and VCA-IgG)	Transiently + 5.9×10^3 (day 14)	− (EA, EBNA2, BZLF1)	245 days (alive)	ND	ND	ND	ND	ND
OK8[b]	IN	3.5×10^8	+ (EA-IgG, VCA-IgM, and VCA-IgG)	Transiently + 3.0×10^2 (day 29)	+ (BZLF1)	168 days (alive)	ND	ND	ND	ND	ND
OK10[b]	IN	9.4×10^8	+ (EA-IgG, VCA-IgM, and VCA-IgG)	Transiently + 2.8×10^2 (day 14)	+ (BZLF1)	20 days (euthanasia)	−	−	+ (a few)	−	+
OK1[c]	PO	1.1×10^9	ND	−	−	74 days (death[f])	−	−	−	−	−
OK2[c]	PO	2.3×10^8	ND	−	−	171 days (euthanasia)	−	−	−	−	−
OK3[c]	PO	2.3×10^8	ND	−	−	119 days (euthanasia)	−	−	−	−	−
OK6[c]	PO	3.2×10^8	−	−	−	224 days (alive)	ND	ND	ND	ND	ND
OK7[c]	PO	4.4×10^8	−	−	−	103 days (euthanasia)	−	−	−	−	−
OK9[c]	PO	1.8×10^9	−	−	−	116 days (alive)	ND	ND	ND	ND	ND
JW[d] (3 cases)	PO and IN	New medium[g]	−	ND	ND	60 days (euthanasia)	−	−	−	−	−

[a]Continuously EBV-DNA-positive rabbit (N = 1).
[b]Transiently EBV-DNA-positive rabbits (N = 3).
[c]EBV-DNA-negative rabbits (N = 6).
[d]Negative control (N = 3).
[f]OK1 died from spinal cord injury in the experiment.
[g]Unused culture medium of RPMI 1640.
ISH, in situ hybridization; IN, intranasal; PO, peroral; PBMCs, peripheral blood mononuclear cells; WBC, white blood cells; RT-PCR, reverse transcriptase-polymerase chain reaction; EBER, EBV-encoded RNA; LMP, latent membrane protein; ZEBRA, *Bam*HI Z fragment Epstein–Barr replication activator; EA, early antigen; ND, not determined; +, positive; −, negative.

J. Med. Virol. DOI 10.1002/jmv

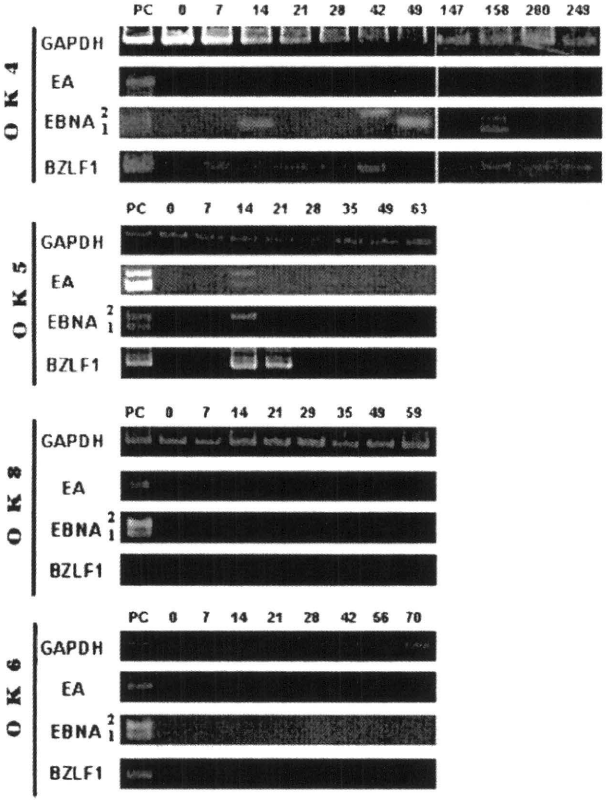

Fig. 2. RT-PCR to detect mRNA expression of EBV-related genes in PBMCs of the rabbits. mRNA of EA, EBNA1, EBNA2, and BZLF1 in PBMCs from the rabbits was determined. In OK4, EBNA, and BZLF1 were detected intermittently from days 14 to 158 and from days 7 to 249, respectively. In OK5, mRNA of *EA* and *EBNA2* were detected only on day 14, and that of BZLF1 was expressed on days 14 and 21. In OK8, only *BZLF1* expression was observed on day 14. In OK10, only BZLF1 expression was positive on day 14 (data not shown). None of these mRNAs were detected in EBV-DNA-negative rabbits (OK6, 7, and 9). The data of OK6 are the representative data of EBV-DNA-negative rabbits. GAPDH was also examined as the internal control.

Histopathological Findings in the Rabbits Inoculated With EBV

OK10, in which EBV-DNA was detected in its PBMCs on day 14, was euthanized and dissected on day 20. Macroscopically, only mild splenomegaly was observed. No pathological abnormality was found on the histological examination of the organs examined by hematoxylin–eosin staining (Fig. 3). However, EBER1-positive lymphocytes were identified in the mesenteric lymph nodes (Fig. 3A-1), spleen (Fig. 3B-1), and tonsils by ISH. Scattered lymphocytes expressed LMP1 or EBNA2 (Fig. 3A-3,B-3) but not ZEBRA in the spleen or lymph nodes. EA expression was also observed in the lymphocytes of the spleen by immunofluorescence staining (Fig. 3C). No EBV-infected EBER1 positive epithelia in the tonsils, liver, and gastrointestinal tract were found by ISH and immunohistochemical staining. In the EBV-DNA-negative rabbits (OK1, OK2, OK3, and OK7) and three negative control rabbits (JW), there were no abnormal pathological findings, and neither EBER1-positive cells nor EBV-related gene protein-expressing cells were observed.

DISCUSSION

There are some advantages in using the rabbit as an animal model for viral infection. Rabbits are easy to care for and to collect blood from the ear vein. They are suitable for observing for prolonged periods. Hayashi et al. [2001, 2003a] reported that HVP-infected rabbits developed fatal hemophagocytic syndrome. HVP is the lymphocryptovirus infecting baboons in nature, and it is similar to EBV biologically and genetically. By using the same animal model, other investigations suggested that the production of anti-red blood cell antibodies and the activation of macrophages are related to the development of EBV-associated hemophagocytic syndrome [Hsieh et al., 2007]. Furthermore, it have been demonstrated recently that EBV can infect the lymphocytes of the Japanese White rabbits by intravenous injection [Takashima et al., 2008]. The inoculated rabbits showed transient mild lymphocytosis, splenomegaly, and uneven echogenecity of the liver by ultrasonography, while immunohistochemistry demonstrated an increase in EBV-VCA antibodies, EBV-DNA detection in PBMCs and plasma, and infiltration of EBER1-positive lymphocytes expressing EBV-related gene proteins in the spleen, lymph nodes, and liver. Therefore, in this study, Japanese White Rabbits were used to develop the animal model of in vivo EBV infection by the oral or nasal route, which resembles the route of primary EBV infection in humans. This primary EBV infection model of the rabbit with intranasal or peroral inoculation showed a lower incidence of infection and mild EBV infection, as compared to the previous model using intravenous EBV inoculation. In this experiment using natural infection routes, detailed EBV antibodies data differed considerably from the known human antibody reaction; and, this study revealed the expression of mRNA of EBV-related genes in PBMCs.

Of 10 rabbits, EBV-DNA was detected in PBMCs of 4 rabbits, all of which were inoculated by the intranasal route. Although EBV is presumed to infect pharyngeal epithelial cells and B-cells in the oral lymphoid tissues including the tonsils by saliva transfer in humans, the exact nature and timing of viral exchange between these tissues and cells has remained controversial [Sixbey et al., 1984; Anagnostopoulos et al., 1995; Niedobitek et al., 1997; Allday and Crawford, 1998]. According to the present data, it may be easier for EBV to infect the rabbit by the intranasal route than the oral route. The rabbits often spat out the inoculated viral solution; also, the tonsils of rabbits are distant anatomically from the orifice of the oral cavity. These seem to be the reasons why the rabbits inoculated perorally with EBV showed a lower incidence of EBV infection (1/7 rabbits) than those inoculated intranasally (4/4 rabbits). EBV may reach directly the pharynx and tonsils with a greater exposure in the case of intranasal inoculation than by the peroral route. In humans, the ability of epithelial cells in vivo

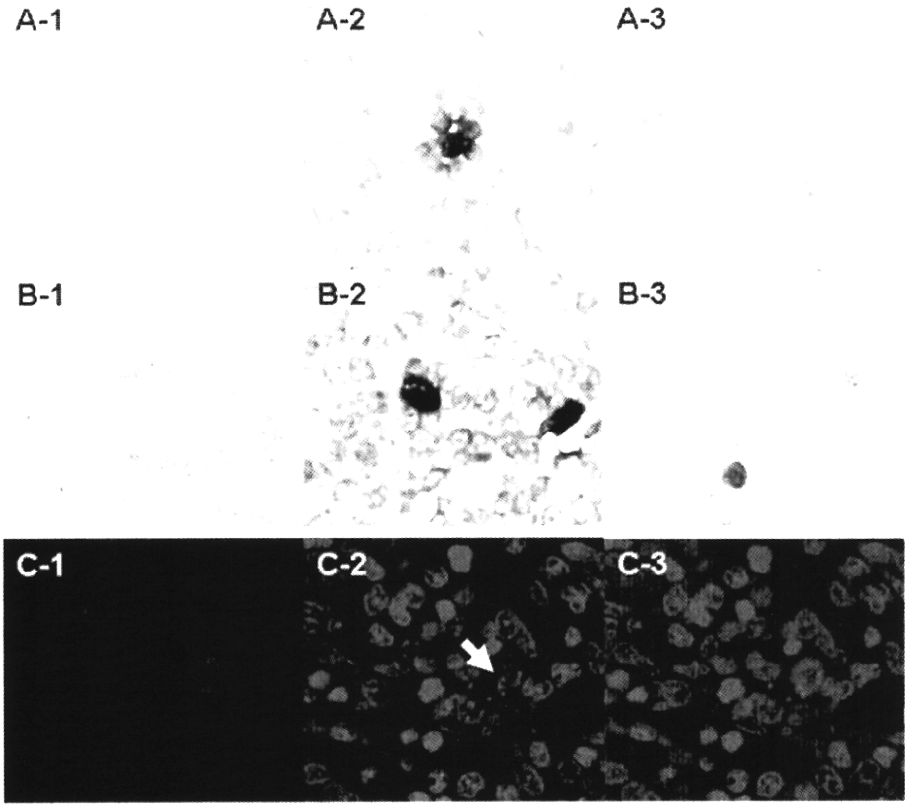

Fig. 3. Histopathological and immunohistochemical analysis and EBER1-ISH in the spleen of OK10. **A**: mesenteric lymph node, (**B** and **C**) spleen. No abnormalities except mild lymphoid hyperplasia were found in the specimens stained with hematoxylin and eosin (A-1,B-1). In the spleen and mesenteric lymph nodes, a few lymphocytes expressed EBER1 by ISH (A-2,B-2) or EBNA2 with immunostaining (A-3,B-3), respectively. The nuclei of some lymphocytes in the spleen were stained brilliantly with green fluorescent color by EA immunofluorescent staining (C-1). However, they showed faint or granular red nuclear staining by propidium iodide (C-2, arrow), indicating dying or apoptotic cells. A merged image is shown in C-3. No pathological abnormalities were found in the tonsils, liver, and terminal ileum. Original magnification was 40× in A-1 and B-1 and 400× in others.

to support latent and lytic infection and the status of memory B-cells as a reservoir for persistent infection go unquestioned with the oral cavity being a site of lifelong periodic EBV shedding [Scott et al., 2005]. In the rabbit experiment, EBV-DNA copies in the saliva from OK4 were shown to be fewer than the threshold level by real-time quantitative PCR assay (unpublished data).

The infection of this model was classified into three types based on the sequential EBV-DNA detection pattern from PBMCs as follows: (1) no EBV-DNA detected (OK1, OK2, OK3, OK6, OK7, and OK9), (2) EBV-DNA continuously detected (OK4), and (3) EBV-DNA detected transiently (OK5, OK8, and OK10). In addition to these three patterns, a pattern detected intermittently was found previously in rabbits inoculated with EBV intravenously [Takashima et al., 2008]. The transition patterns of the EBV-DNA quantity in PBMCs in this model using intranasal or peroral inoculation resemble those of the model using intravenous injection.

The time courses of the four types of EBV antibody titers in the infected rabbits differed considerably from those in humans. In primary EBV infection in humans, EA-IgG levels are elevated only during the acute phase [Bauer, 2001], whereas EA-IgG levels of EBV-infected rabbits increased rapidly during the early phase and high titers were maintained continuously regardless of copy numbers of EBV-DNA in the blood. The elevation of VCA-IgG, which is continuous from the acute phase in humans [Schillinger et al., 1993], was transient in the rabbits in this experiment, but the VCA-IgG titer measured by immunofluorescence was increased for over 1 year in the previous report [Takashima et al., 2008]. EBNA-IgG, which is elevated during the convalescence period of EBV primary infection and maintained at high levels in humans [Henle et al., 1987; Schillinger et al., 1993], was not elevated in the rabbits during the observation period of up to 396 days. However, very low-level increases in EBNA-IgG were observed in some of the rabbits infected by intravenous injection of EBV after 600 days [unpublished data of Takashima et al., 2008]. Although the elevation of EA-IgG reflects generally the acute phase or exacerbation (reactivated phase) of EBV infection in humans, EBV-positive rabbits, regardless of EA-IgG titers, did not show any symptoms or remarkable abnormalities in the blood. In addition, high EA-IgG levels continued after infection

during the observation period, even when EBV-DNA copy numbers of EBV-positive rabbits were decreased or were undetectable. These observations suggest that the immune responses of the rabbit to EBV differ considerably from those of humans, but it is difficult currently to clarify whether this difference is related to the low virulence of EBV to rabbits. It is necessary to elucidate the function of antibodies against EA, VCA, and EBNA in rabbits in vivo. ELISA kits used in this study were developed for the examination of human sera. However, the specificity of these ELISAs was shown in this study, replacing the secondary antibody to HRP-conjugated anti-rabbit IgG or IgM, because anti-EBV reaction or increased antibody titers to EBV were demonstrated only in EBV-DNA positive rabbits, but not in EBV-DNA negative rabbits.

According to the results of RT-PCR using PBMCs, mRNA of EA was detected only in OK5 on day 14, although EA-IgG levels were high in all the EBV-positive rabbits. That is the possible reason why mRNA expression levels in PBMCs may be very low or lower than the detection sensitivity. However, it was confirmed that EA was expressed also in the spleen by immunofluorescent examination. BZLF1 induces the reactivation of EBV [Tsurumi et al., 2005]. BZLF1 mRNA was expressed for more than 8 months after EBV inoculation in OK4, whereas it was detected only on days 14 and 21 in OK5, and on day 14 in OK8 and OK10. BZLF1 mRNA expression was observed only when EBV-DNA could be detected in PBMCs. Although EBNA1 and EBNA2 are important genes for the development of latent infection [Tsurumi et al., 2005], they were detected intermittently or transiently from 2 weeks after EBV inoculation in EBV-positive rabbits. In the histopathological investigation, EBER1-, EBNA2-, or LMP1-positive lymphocytes and EA-expressing cells were found; however, ZEBRA expression was not observed in different lymphoid tissues, which is compatible with latency 2, 3, or lytic infection. In the previous report, spleen lymphocytes of rabbits inoculated with EBV also expressed these latent infection markers or the lytic infection marker (ZEBRA). However, these EBV-marker-positive lymphocytes were present in smaller numbers in this experiment. These findings suggest that intranasal or peroral inoculation of EBV can induce primary EBV infection in some rabbits: however, latent EBV infection of type 1 in humans could not be shown or confirmed in this experiment. It appears difficult for EBV to change from a transient lytic infection to a latent infection in most rabbits. The immune system of the rabbit may respond strongly to expressed EBV-related gene proteins and lead to the elimination of the virus from the rabbits. Alternatively, there may be unknown agents in the lymphocytes of the rabbit that inhibit the development of latent infection. The details of these factors that eliminate EBV could lead to the discovery of therapeutic or preventive measures against EBV-related disease. EBV-DNA was detected for a long period in some of the rabbits inoculated with EBV (OK4 in this study and TJ-16 in our previous report Takashima et al., 2008), mimicking chronic active EBV infection. Although some rabbits may have a type of immunodeficiency against EBV, it is unclear why they could not eliminate EBV promptly.

In conclusion, EBV can infect the rabbit by the intranasal or peroral route, and rabbits inoculated with EBV by these airway routes are a convenient and interesting animal model for examining the pathophysiology of natural primary EBV infection in humans. Tracing and analyzing the EBV dynamics with time and clarifying the location and manner of EBV proliferation after intranasal or peroral infection are expected to be useful. This model can be applied for the development of vaccines or treatments.

REFERENCES

Allday MJ, Crawford DH. 1998. Role of epithelium in EBV persistence and pathogenesis of B-cell tumours. Lancet 1:855–857.

Anagnostopoulos I, Hummel M, Kreschel C, Stein H. 1995. Morphology, immunophenotype, and distribution of latently and/or productively Epstein-Barr virus-infected cells in acute infectious mononucleosis: Implications for the interindividual infection route of Epstein-Barr virus. Blood 85:744–750.

Aozasa K. 1996. Pyothorax-associated lymphoma. Int J Hematol 65:9–16.

Bauer G. 2001. Simplicity through complexity: Immunoblot with recombinant antigens as the new gold standard in Epstein-Barr virus serology. Clin Lab 47:223–230.

Bear R, Bankier AT, Biggin MD, Deininger PL, Farrell PJ, Gibson TJ, Hatfull G, Hudson GS, Satchwell SC, Tuffnell PS, Barrell BG, Séguin C. 1984. DNA sequence and expression of the B 95-8 Epstein -Barr virus genome. Nature 310:207–211.

Bergallo M, Costa C, Baro S, Musso T, Balbo L, Merlino C, Cavallo R. 2007. Multiplex-nested RT-PCR to evaluate latent and lytic Epstein Barr virus gene expression. J Biothechnol 128:462–476.

Chang KL, Chen YY, Shibata D, Weiss LM. 1992. Description of an in situ hybridization methodology for detection of Epstein-Barr virus RNA in paraffin-embedded tissues, with a survey of a normal and neoplastic tissues. Diagn Mol Pathol 1:246–255.

Cocco M, Bellan C, Tussiwand R, Corti D, Traggiai E, Lazzi S, Mannucci S, Bronz L, Palummo N, Ginanneschi C, Tosi P, Lanzavecchia A, Manz MG, Leoncini L. 2008. CD34 + cord blood cell-transplanted Rag2 / gamma(c) - / - mice as a model for Epstein-Barr virus infection. Am J Pathol 173:1369–1378.

Cohen JI. 2000. Epstein-Barr virus infection. N Engl J Med 343: 481–492.

Epstein MA, Achong BG, Barr YM. 1964. Virus particles in culutured lymphoblasts from Barkitt's lymphoma. Lancet 15: 702–703.

Epstein MA, zur Hausen H, Ball G, Rabin H. 1975. Pilot experiments with EB virus in owl monkeys (Aotus trivirgatus). III. Serological and biochemical findings in an animal with reticuloproliferative disease. Int J Cancer 15:17–22.

Hayashi K, Ohara N, Teramoto N, Onoda S, Chen HL, Oka T, Kondo E, Yoshino T, Takahashi K, Yates J, Akagi T. 2001. An animal model for human EBV-associated hemophagocytic syndrome: Herpesvirus papio frequently induces fatal lymphoproliferative disorders with hemophagocytic syndrome in rabbits. Am J Pathol 158:1533–1542.

Hayashi K, Jin Z, Onoda S, Joko H, Teramoto N, Ohara N, Oda W, Tanaka T, Liu XY, Koirala TR, Oka T, Kondo E, Yoshino T, Takahashi K, Akagi T. 2003a. Rabbit model for human EBV-associated hemophagocytic syndrome (HPS): Sequential autopsy analysis and characterization of IL-2-dependent cell lines established from herpesvirus papio-induced fatal rabbit lymphoproliferative diseases with HPS. Am J Pathol 162:1721–1736.

Hayashi K, Joko H, Koirala TR, Onoda S, Jin ZS, Munemasa M, Ohara N, Oda W, Tanaka T, Oka T, Kondo E, Yoshino T, Takahashi K, Yamada M, Akagi T. 2003b. Therapeutic trials for a rabbit model of EBV-associated Hemophagocytic Syndrome (HPS): Effects of vidarabine or CHOP, and development of Herpesvirus papio (HVP)-negative lymphomas surrounded by HVP-infected lymphoproliferative disease. Histo. Histopatho. 18:1155–1168.

Henle W, Henle G, Anderson J, Emberg I, Klein G, Horwitz CA, Markland G, Rymo L, Wellinder C, Straus SE. 1987. Antibody responses to Epstein-Barr virus-determined nuclear antigen (EBNA)-1 and EBNA-2 in acute and chronic Epstein-Barr virus infection. Proc Natl Acad Sci USA 84:570–574.

Hsieh WC, Chang Y, Hsu MC, Lan BS, Hsiao GC, Chuang HC, Su IJ. 2007. Emergence of anti-red blood cell antibodies triggers red cell phagocytosis by activated macrophage in a rabbit model of Epstein-Barr virus-associated hemophagocytic syndrome. Am J Pathol 170: 1629–1639.

Imashuku S. 2002. Clinical features and treatment strategies of Epstein-Barr virus-associated hemophagocytic lymphohistiocytosis. Crit Rev Oncol Hematol 44:259–272.

Isaacson P, Wright DH. 1983. Malignant lymphoma of mucosa-associated lymphoid tissue: A distinct type of B-cell lymphoma. Cancer 52:1410–1416.

Johannessen I, Crawford DH. 1999. In vivo models for Epstein-Barr virus (EBV)-associated B cell lymphoproliferative disease (BLPD). Rev Med Virol 9:263–277.

Kimura H, Morita M, Yabuta Y, Kuzushima K, Kato K, Kojima S, Matsuyama T, Morishima T. 1999. Quantitative analysis of Epstein-Barr virus load by using a real-time PCR assay. J Clin Microbiol 37:132–136.

Kimura H, Ito Y, Suzuki R, Nishiyama Y. 2008. Measureing Epstein-Barr virus (EBV) load: The significance and application for each EBV-associated disease. Rev Med Virol 18:305–319.

Melkus MW, Estes JD, Padgett-Thomas A, Gatlin J, Denton PW, Othieno FA, Wege AK, Haase AT, Garcia JV. 2006. Humanized mice mount specific adaptive and innate immune responses to EBV and TSST-1. Nat Med 12:1316–1322.

Mosier DE, Gulizia RJ, Baird SM, Wilson DB. 1988. Transfer of a functional human immune system to mice with severe combined immunodeficiency. Nature 335:256–259.

Niedobitek G, Agathanggelou A, Herbst H, Whitehead L, Wright DH, Young LS. 1997. Epstein-Barr virus (EBV) infection in infectious mononucleosis: Virus latency, replication and phenotype of EBV-infected cells. J Pathol 182:151–159.

Rivailler P, Carville A, Kaur A, Rao P, Quink C, Kutok JL, Westmoreland S, Klumpp S, Aster JC, Wang F. 2004. Experimental rhesus lymphocryptovirus infection in immunosuppressed macaques: An animal model for Epstein-Barr virus pathogenesis in the immunosuppressed host. Blood 104:1482–1489.

Schillinger M, Kampmann M, Henninger K, Murray G, Hanselmann I, Bauer G. 1993. Variability of humoral immune response to acute Epstein-Barr virus (EBV) infection: Evaluation of the significance of serological markers. Med Microbiol Lett 2:296–303.

Scott RS, Moody CA, Sixbey JW. 2005. In: Robertson ES, editor. Epstein-Barr virus and oral malignancy. England: Caister Academic Press. pp 55–70.

Shope T, Dechairo D, Miller G. 1973. Malignant lymphoma in cottontop marmosets after inoculation with Epastein-Barr virus. Proc Natl Acad Sci 70:2487–2491.

Sixbey JW, Nedrud JG, Raab-Traub N, Hanes RA, Pagano JS. 1984. Epstein-Barr virus replication in oropharyngeal epithelial cells. N Engl J Med 10:1225–1230.

Straus SE. 1988. The chronic mononucleosis syndrome. J Infect Dis 157:405–412.

Straus SE, Cohen JI, Tosato G, Meier J. 1993. NIH conference: Epstein-Barr virus infections: Biology, pathology, and management. Ann Intern Med 118:45–58.

Sugimoto M, Tahara H, Ide T, Furuichi Y. 2004. Steps involved in immortalization and tumorigenesis in human B-lymphoblastoid cell lines transformed by Epstein-Barr virus. Cancer Res 64: 3361–3364.

Takashima K, Ohashi M, Kitamura Y, Ando K, Nagashima K, Sugihara H, Okuno K, Sairenji T, Hayashi K. 2008. A new animal model for primary and persistent Epstein-Barr virus infection: Human EBV-infected rabbit characteristics determined using sequential imaging and pathological analysis. J Med Virol 80:455–466.

Tsurumi T, Fujita M, Kudoh A. 2005. Latent and lytic Epstein-Barr virus replication strategies. Rev Med Virol 15:3–15.

Williams H, Crawford DH. 2006. Epstein-Barr virus: The impact of science advances on clinical practice. Blood 107:862–869.

Yajima M, Imadome K, Nakagawa A, Watanabe S, Terashima K, Nakamura H, Ito M, Shimizu N, Honda M, Yamamoto N, Fujiwara S. 2008. A new humanized mouse model of Epstein-Barr virus infection that reproduces persistent infection, lymphoproliferative disorder, and cell-mediated and humoral immune responses. J Infect Dis 198:673–682.

Biomedical Research 31 (4) 219-230, 2010

Effects of cyclohexenonic long-chain fatty alcohol in type 2 diabetic rat nephropathy

Shinichi OKADA[1], Motoaki SAITO[2], Yukako KINOSHITA[2], Itaru SATOH[2], Yasuo KAWABA[1], Atsushi HAYASHI[1], Takashi OITE[3], Keisuke SATOH[2], and Susumu KANZAKI[1]

[1] Division of Pediatrics and Perinatology, Tottori University Faculty of Medicine, 36-1 Nishi-cho, Yonago, 683-8504; [2] Division of Molecular Pharmacology, Tottori University Faculty of Medicine, 86 Nishi-cho, Yonago, 683-8503; and [3] Department of Cellular Physiology, Institute of Nephrology, Niigata University Graduate School of Medical and Dental Sciences, 1-757 Asahimachi-dori, Chuo-ku, Niigata, 951-8150, Japan

(Received 13 April 2010; and accepted 14 May 2010)

ABSTRACT

We attempted to clarify the effects of cyclohexenonic long-chain fatty alcohol (CHLFA) on the alterations of type 2 diabetes-induced nephropathy. Forty-week-old male Goto-Kakizaki (GK) and Wistar rats were divided into four groups of 6 to 8 animals. Group A consisted of eight Wistar rats and served as an age-matched control group. Group B (7 GK rats) received no treatment and served as a diabetic group. Group C (6 GK rats) was treated daily with low-dose CHLFA (2 mg/kg/body weight, subcutaneously) for 30 weeks, and Group D (6 GK rats) with high-dose CHLFA (8 mg/kg/body weight) for 30 weeks. At the end of the treatment period, urinary protein excretion, blood chemistry, renal histological, and immunohistological analyses were conducted. Although CHLFA administration did not influence serum glucose or insulin levels, it reversed diabetes-induced increases in urinary protein excretion and serum creatinine. Light microscopically, CHLFA treatment ameliorated the otherwise elevated glomerular sclerotic scores in the diabetic group. Immunohistochemically, increased expression of desmin and decreased expression of rat endothelial cell antigen-1 in the group with untreated diabetes both showed a reversal to control levels in the high-dose CHLFA treatment group. In conclusion, CHLFA may ameliorate type 2 diabetes-induced nephropathy.

Recently, diabetic nephropathy with type 2 diabetes has become the most common cause of end-stage renal disease. To inhibit the progression of diabetic vascular diseases, therapeutic agents such as renin-angiotensin II system (RAS) inhibitors, radical scavengers (6) and PKC-β inhibitors (12) have been investigated. However, in order to prevent diabetes-induced complications, the development of other therapeutic agents will still be necessary.

The Goto-Kakizaki (GK) rat represents a spontaneous non-insulin-dependent diabetes model. GK rats are produced from normal Wistar rats by repeated selective breeding, and they are widely accepted as a genetically determined rodent model of human type 2 diabetes. This genetic rat model is particularly relevant for human type 2 diabetes research, because defects in glucose-stimulated insulin secretion, peripheral insulin resistance, and hyperinsulinemia are seen as early as four weeks after birth, and later-onset abnormalities include hypoinsulinemia and modest hyperglycemia (14).

The tropical plant, *Hygrophilia erecta Hochr.*, has been shown to contain certain cyclohexenonic long-chain fatty alcohols (CHLFAs) that exhibit a

Address correspondence to: Motoaki Saito, MD, PhD
Department of Pathophysiological and Therapeutic Science, Division of Molecular Pharmacology, Tottori University Faculty of Medicine, 86 Nishi-cho, Yonago 683-8503, Japan
Tel: +81-859-38-6162, Fax: +81-859-38-6160
E-mail: saitomo@med.tottori-u.ac.jp

neurotrophic activity on cultured neurons from the cerebral cortex (2, 3). CHLFA has been found to directly increase neurite extension as well as to enhance the biochemical differentiation of these neurons. We previously reported that CHLFA prevented the progression of diabetes-induced alterations in the trachea, aorta, and urinary bladder (22, 24, 25). Moreover, our previous reports demonstrated that CHLFA ameliorates the progression of diabetes-induced nephropathy in streptozotocin (STZ)-induced diabetic rats (17, 21). Whereas CHLFA did not ameliorate the general features of diabetes, elevated serum glucose or decreased insulin levels in the STZ-induced diabetic rats, it did significantly prevent the progression of glomerulosclerosis. Based on the findings of these earlier studies, we propose that CHLFA may prevent not only type 1 diabetes-induced nephropathy, but also type 2 diabetes-induced nephropathy; furthermore, these preventive effects appear to take place in a manner independent of serum insulin and glucose levels.

Therefore, the aims of the present study were to investigate a feature of type 2 diabetes-induced nephropathy, and to clarify the possible ameliorative effects of CHLFA on type 2 diabetes-induced nephropathy.

MATERIALS AND METHODS

Animal models. All animal experiments were performed in accordance with the guidelines established by the Tottori University Committee for Animal Experimentation. Six-week-old male GK and Wistar rats were purchased from SLC (Shizuoka, Japan). All rats were kept under identical conditions, and all had access to food and drinking water *ad libitum*. At the age of 40 weeks, the rats were divided randomly into four groups (n = 7–8 each): age-matched Wistar rats administered vehicle (A), diabetic GK rats administered vehicle (B), diabetic GK rats treated with cyclohexenonic long-chain fatty alcohol (CHLFA; 2,4,4-trimethyl-3-[15-hydroxypentadecyl]-2-cyclohexen-1-one [Meiji Milk Products Co., Ltd., Tokyo, Japan]) at a daily dose of 2 mg/kg (C), and diabetic GK rats treated with CHLFA at a daily dose of 8 mg/kg (D) intramuscularly. CHLFA was dissolved in ethanol, and a mixture of physiological saline/Tween 80 was added at a ratio of ethanol: saline: Tween 80 = 5 : 92.15 : 2.85 (total volume: 1 mL/kg). Drug or vehicle administration was initiated when each rat had reached the age of 40 weeks. Upon reaching 70 weeks of age, the rats were sacrificed with an overdose of pentobarbital (60 mg intraperitoneally) after twenty-four hours of fasting. Immediately thereafter, blood samples were collected from the vena cava, and the renal tissues were removed. The blood samples and kidneys were frozen at −80°C until use.

Measurement of urinary excretion and protein excretion. Over one 24-hour period between days 489 and 490 (week 70), the rats were placed in a metabolic cage containing a urine-collection funnel over an electronic balance (HL200; A.N.D., Tokyo, Japan) to measure urine excretion. Sesame oil (Nisshin OilliO Group, Ltd., Tokyo, Japan) was used to prevent evaporation of the urine during collection. The balances were connected to a personal computer (Macintosh Power Book G4; Apple Computer, Cupertino, CA) via a multiport controller (PowerLab/8sp; AD Instruments, Castle Hill, Australia) to monitor the cumulative weight of the collected urine. All rats received food and water *ad libitum* in the cage. Each monitoring period started at 18 : 00, and urine was collected for exactly 24 h. Then, the total urine excretion of the rats was determined. After the urine of each animal had been collected, the urinary levels of protein were determined using an enzyme-linked immunosorbent assay (ELISA) kit (Protein Assay Rapid Kit Wako; Wako Pure Chemical Industries, Osaka, Japan) according to the manufacturer's instructions.

Serum glucose, insulin, creatinine, and blood urea nitrogen measurement. The serum glucose, insulin, creatinine, and blood urea nitrogen concentrations of experimental rats were measured by the hexokinase method (Glucose C II; Wako Pure Chemical Industries), the ELISA method (Rat Insulin ELISA; Mercodia AB, Uppsala, Sweden), the Jaffe method (Creatinine-test Wako; Wako Pure Chemical Industries), and the urease-indophenol method (Urea N B; Wako Pure Chemical Industries), respectively, all of which were carried out according to the kit manufacturers' instructions.

Histological examination of the rat kidney. The right kidney was immediately fixed with 10% formalin. After fixation, the tissues were embedded in paraffin, and 5-μm-thick tissue sections were cut from the paraffin blocks. All of the kidney specimens were stained using hematoxylin and eosin (H & E) and periodic acid-Schiff (PAS). Each section was viewed under a light microscope at a magnification of ×100–400. Histological evaluation was performed without knowledge of the identity of the various

groups. In the PAS-stained sections, approximately 100 glomeruli in a specimen (n = 8, 7 , 7, or 7 per group, respectively) were evaluated by one pathologist and one nephrologist, and mesangial matrix expansion and glomerular sclerosis were graded semiquantitatively on a scale of 0 to 4+ according to the method described by Raij *et al.* (19). The areas used for evaluation were randomly selected, and the values were expressed as per high-powered field (HPF). The numbers of glomeruli with nodule-like lesions were counted, and these values were normalized with the number of glomeruli counted.

Immunohistochemical analysis of the rat kidney. The serial sections of the kidney were also subjected to immunohistochemical staining for α-smooth muscle cell actin (α-SMA), desmin, ED-1, and collagen type IV. Briefly, after the sections were deparaffinized, they were then reacted overnight with anti-α-SMA, anti-desmin (Abcam Ltd., Cambridge, UK), anti-ED-1 (AbD Serotec Ltd., Kidlington, UK) or anti-collagen type IV polyclonal primary antibody (Progen Biotechnik GmbH, Heidelberg, Germany) at a 1 : 100, 1 : 200, 1 : 100 or 1 : 50 dilution, respectively. The specifically bound first antibodies were visualized by a secondary antibody conjugated with peroxidase using Histofine simple stain (rat MAX-PO) (Nichirei Co., Tokyo, Japan) with a Histofine simple stain substrate (Nichirei Co.). Mayer's hematoxylin was used for counterstaining. Negative controls were established for each group according to the procedure of immunohistochemical staining mentioned above, but without a secondary antibody conjugated with peroxidase. Immunohistochemical evaluation was performed without knowledge of the identity of the various groups. In each of the stained sections, approximately 100 randomly selected glomeruli or a field of 20 tubulointerstitial areas were analyzed in each specimen (group A, B, C and D: n = 8, 7, 7 and 7, respectively) by one pathologist and one nephrologist, and immunostaining of the glomerular area and tubulointerstitial grid field were graded semiquantitatively on a scale of 0 to 4+ according to the method of Janssen *et al.* (7).

Immunofluorescent microscopy of the rat kidney using frozen sections. To assess the glomerular nodule-like lesions, immunofluorescent double-label staining for platelet-endothelial cell adhesion molecule-1 (PECAM-1; CD-31) and Thy1 antigen (OX-7) was evaluated in group B. Frozen tissue sections were incubated with mouse monoclonal antibody against rat PECAM-1(Serotec Ltd., Kidlington, UK) as a primary antibody, followed by incubation with FITC-labeled rabbit anti-mouse immunoglobulins (Dako Denmark A/S, Glostrup, Denmark) as a secondary antibody. Then, the sections were incubated with biotinylated mouse antibody against rat OX-7 (Abcam) for identifying glomerular mesangial cells, followed by incubation with tetramethyl rhodamine B isothiocyanate-conjugated streptavidin (KPL Inc., Gaithersburg, MD). Stained sections were examined with confocal laser scanning immunofluorescent microscopy (MRC-1024; Bio-Rad Laboratories, Hemel Hempstead, UK).

Serial sections of tissue were also subjected to immunofluorescent double-label staining for rat endothelial cell antigen-1 (RECA-1) and Thy1 antigen (OX-7) for further evaluation. Monoclonal mouse anti-RECA-1 antibody was obtained from AbD Serotec. The secondary antibodies were FITC-conjugated rabbit anti-mouse immunoglobulin (Dako Denmark A/S) for the anti-RECA-1 antibody, and TRITC-conjugated anti-mouse immunoglobulin (Dako Denmark A/S) for the anti-OX-7 antibody. In the immunofluorescent-stained sections, approximately 3 to 13 glomeruli in a specimen (n = 4, 4, 4, or 3 per group, respectively) were evaluated by one pathologist and one nephrologist, and the expansion scores based on immunofluorescent staining were graded semiquantitatively on a scale of 0 to 4+.

Data analysis. All data were evaluated by parametric ANOVA and expressed as the means ± S.E.M. Statistical analyses were conducted using the Tukey-Kramer Test for multiple comparisons and Kyplot software. Student's t-test was used for comparison of urinary albumin excretion and for biochemical serum analyses. For all statistical tests, a P-value of less than 0.05 indicated statistical significance.

RESULTS

General features of experimental rats

General features of each group are shown in Table 1. By the age of 40 weeks, GK diabetic rats showed a significantly smaller amount of weight gain than their non-diabetic counterparts, and these rats also showed no weight gain during the experimental period. The kidney weight and the kidney weight/body weight ratio of GK diabetic rats significantly increased. Treatment with CHLFA neither increased the body weight gain nor decreased the kidney weight/body weight ratio. Moreover, GK diabetic rats had significantly higher serum glucose levels and lower serum insulin levels than control rats (Ta-

ble 2). Treatment with CHLFA had no effect on either serum glucose or insulin levels. The GK diabetic rats also exhibited increased levels of serum creatinine and urinary protein excretion, as compared to those of control rats. CHLFA had no effect on blood urea nitrogen levels, but high-dose (8 mg/kg) CHLFA improved serum creatinine and urinary protein excretion levels compared to those of untreated GK rats (Table 2).

Histological examination of the rat kidney

Fig. 1 shows PAS-stained specimens of all groups, and Fig. 2 shows the mesangial matrix expansion scores and glomerular sclerosis scores. In the untreated GK rat group (group B), mesangial matrix expansion and segmental glomerular sclerosis were evident. The mesangial matrix expansion scores in Figs. 1A, B, C, and D were 1+, 4+, 2+, and 1+, respectively. On the other hand, the glomerular sclerosis scores in Figs. 1A, B, C, and D were 0, 3+, 1+, and 1+, respectively. Treatment with CHLFA significantly ameliorated diabetes-induced alteration of the kidney. The mesangial matrix expansion scores and glomerular sclerosis scores of untreated GK rats (group B) were significantly higher than those of control rats (group A) (Fig. 2). Although the findings did not reach the level of statistical significance, CHLFA appeared to inhibit the progression of glomerular sclerosis in a dose-dependent manner and tended to reverse mesangial matrix expansion.

Glomeruli with segmental nodule-like lesions (Figs. 1B, 1C, and 1D) similar to nodular Kimmelstiel-Wilson lesions were observed in all groups. The scores in the untreated GK rats (group B) were significantly higher than those of the control group (Fig. 3). Although the association was not statistically significant, CHLFA tended to be associated with scores approaching normal levels.

Immunohistochemical analysis of the rat kidney

Immunostaining for α-SMA, a marker of activated mesangial cells (8), in the glomeruli did not differ among groups (Fig. 4). The glomerular expression of desmin, a marker of injured podocytes (4, 32), was significantly higher in untreated GK rats (group B) than in control rats (group A), and CHLFA inhibited the expression of desmin in a dose-dependent manner (Figs. 4 and 6). Fig. 6B shows an accumulation of desmin in the podocyte region, and this accumulation was significantly lower in group D. Although the findings did not reach the level of significance, the expression of ED-1, a marker of monocyte/macrophage infiltration into glomeruli, was upregulated in untreated GK rats (group B),

Table 1 *The general features in the experimental rats*

	Body weight (g)		Kidney weight (g)	Kidney weight (mg)/ body weight (g)
	Age 40 weeks	Age 70 weeks		
A	535.6 ± 19.8	546.3 ± 20.0	1.40 ± 0.04	2.58 ± 0.06
B	419.3 ± 4.0*	394.3 ± 3.7*	1.59 ± 0.04*	4.01 ± 0.08*
C	416.4 ± 8.3*	400.0 ± 8.7*	1.65 ± 0.06*	4.18 ± 0.14*
D	409.3 ± 5.6*	387.1 ± 8.1*	1.53 ± 0.05	3.96 ± 0.16*

A: control rats. B: diabetic rats, C: diabetic rats treated with 2 mg/kg cyclohexenonic long-chain fatty alcohol (CFLFA), and D: diabetic rats treated with 8 mg/kg CHLFA.
Data are shown as mean ± S.E.M. of six to eight separated determinations in each group.
*Significantly different from group A. ($P < 0.05$)

Table 2 *The experimental data in the rats*

	Serum glucose (mg/dL)	Serum insulin (μg/L)	Urinary excretion (mL/day)	Serum BUN (mg/dL)	Serum creatinine (mg/dL)	Protein excretion (mg/24 h)
A	132.2 ± 5.9	2.51 ± 0.33	12.7 ± 1.3	21.8 ± 1.9	0.78 ± 0.09	88.7 ± 23.4
B	208.1 ± 8.5*	0.53 ± 0.10*	13.2 ± 1.5	22.7 ± 1.3	0.99 ± 0.04*	221.1 ± 38.4*
C	217.3 ± 16.4*	0.54 ± 0.10*	14.1 ± 2.9	24.0 ± 1.0	0.99 ± 0.08*	209.4 ± 24.5*
D	209.1 ± 6.1*	0.94 ± 0.15*	15.3 ± 1.3	20.8 ± 1.1	0.92 ± 0.05	171.0 ± 30.4

A: control rats. B: diabetic rats. C: diabetic rats treated with 2 mg/kg cyclohexenonic long-chain fatty alcohol (CHLFA), and D: diabetic rats treated with 8 mg/kg CHLFA.
Data are shown as mean±S.E.M. of six to eight separated determinations in each group.
*Significantly different from group A. ($P < 0.05$)

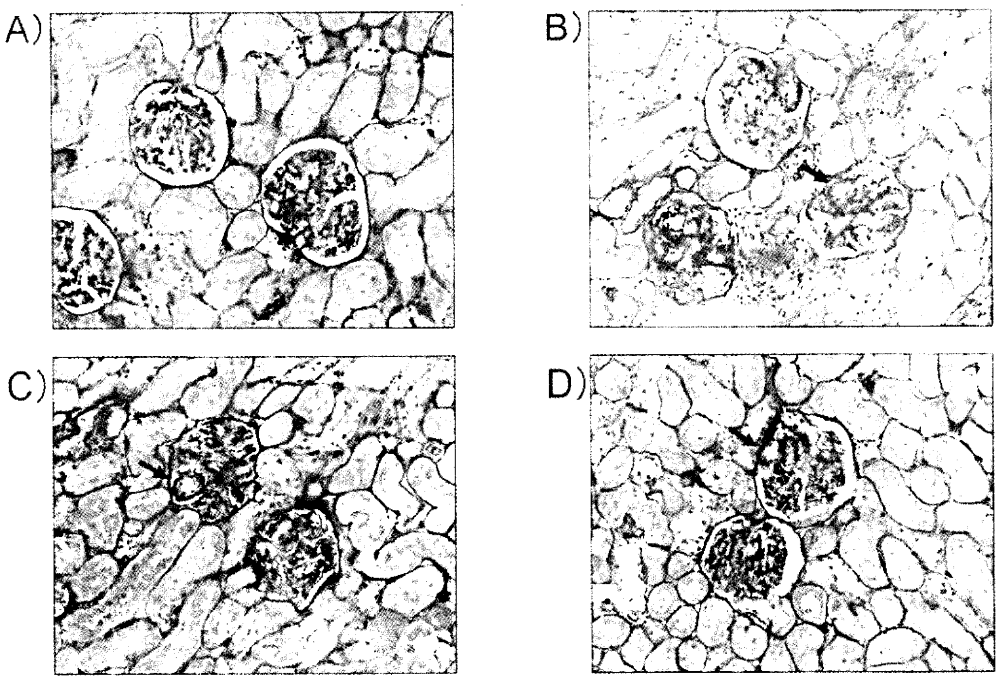

Fig. 1 Histological examination of the kidney. A: Wistar rats, B: GK rats treated with vehicle, C: GK rats treated with 2 mg/kg of cyclohexenonic long-chain fatty alcohol (CHLFA), and D: GK rats treated with 8 mg/kg of CHLFA. Severe mesangial matrix expansion and segmental glomerular sclerosis are observed in the untreated GK rat group (B). Glomeruli with segmental nodule-like lesions are observed (arrows). (×400 magnification)

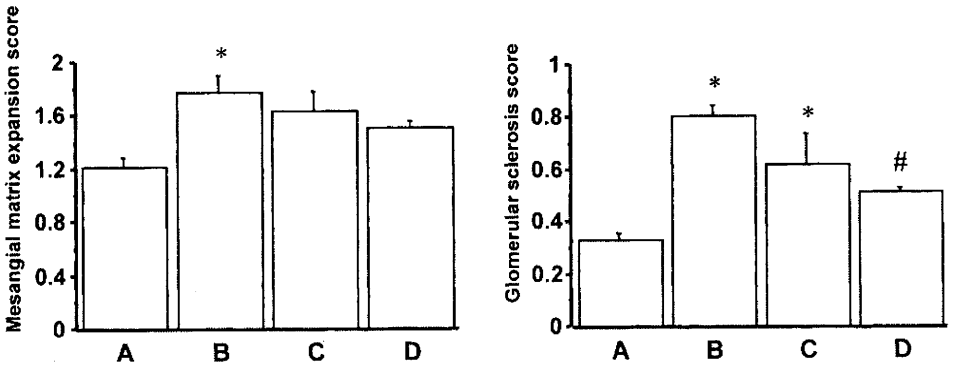

Fig. 2 Histological evaluation of the kidney for mesangial matrix expansion score and glomerular sclerosis score. A: Wistar rats, B: GK rats treated with vehicle, C: GK rats treated with 2 mg/kg of cyclohexenonic long-chain fatty alcohol (CHLFA), and D: GK rats treated with 8 mg/kg of CHLFA. Data are shown as the means ± S.E.M. of five separate determinations in each group. *: Significantly different compared to group A ($P < 0.05$). #: Significantly different compared to group B ($P < 0.05$).

and tended to be lower in groups C and D in a dose-dependent manner (Fig. 4). On the other hand, glomerular collagen type IV expression did not differ among the groups (Fig. 4).

In the renal tubules and the peritubular interstitium, the levels of expression of α-SMA, a marker of myofibroblasts in the interstitium, and ED-1, a marker of monocyte/macrophage infiltration into the interstitium in the untreated GK rats (group B) tended to increase as compared to those of control rats (group A) (Fig. 5). In contrast, the level of collagen type IV, a marker of fibrosis of the interstitium, in the untreated GK rats (group B) significantly increased as compared to those of control rats (group

A) (Fig. 5). Treatment with high-dose CHLFA decreased the expression of these markers, albeit not significantly. Low levels of desmin expression were seen in all groups (data not shown).

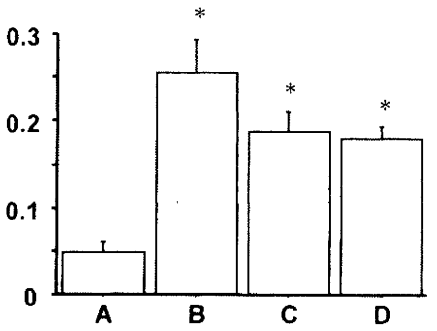

Fig. 3 Histological evaluation of nodule-like lesions. A: Wistar rats, B: GK rats treated with vehicle, C: GK rats treated with 2 mg/kg of cyclohexenonic long-chain fatty alcohol (CHLFA), and D: GK rats treated with 8 mg/kg of CHLFA. Data are shown as the means ± S.E.M. of five separate determinations in each group. *: Significantly different compared to group A ($P < 0.05$).

Immunofluorescent microscopic analysis of frozen sections of the rat kidney

Anti-CD-31 antibody and anti-OX-7 antibody respectively reacted with endothelial cells of the glomerular capillary and mesangial cells. Positive staining with both antibodies was observed in the glomeruli (Fig. 7). CD-31 staining in the glomeruli surrounded nodule-like lesions, and negative internal staining of the nodule-like lesions was also observed (Fig. 7). On the other hand, OX-7-positive staining was observed in the nodule-like lesions, as shown in the merged images (Fig. 7).

Fig. 8 shows the results of immunostaining for RECA-1 or OX-7 in all groups, and Fig. 9 shows the expansion scores based on immunofluorescent stainings. Immunostaining for RECA-1 in untreated GK rats (group B) (Fig. 8d) revealed that the number of RECA-1-positive capillaries decreased as compared to that in control rats (group A) (Fig. 8a), and capillary density had recovered to normal in group D (Figs. 8j and 9), although neither result was statistically significant. On the other hand, immunostaining for OX-7 in untreated GK rats (group B)

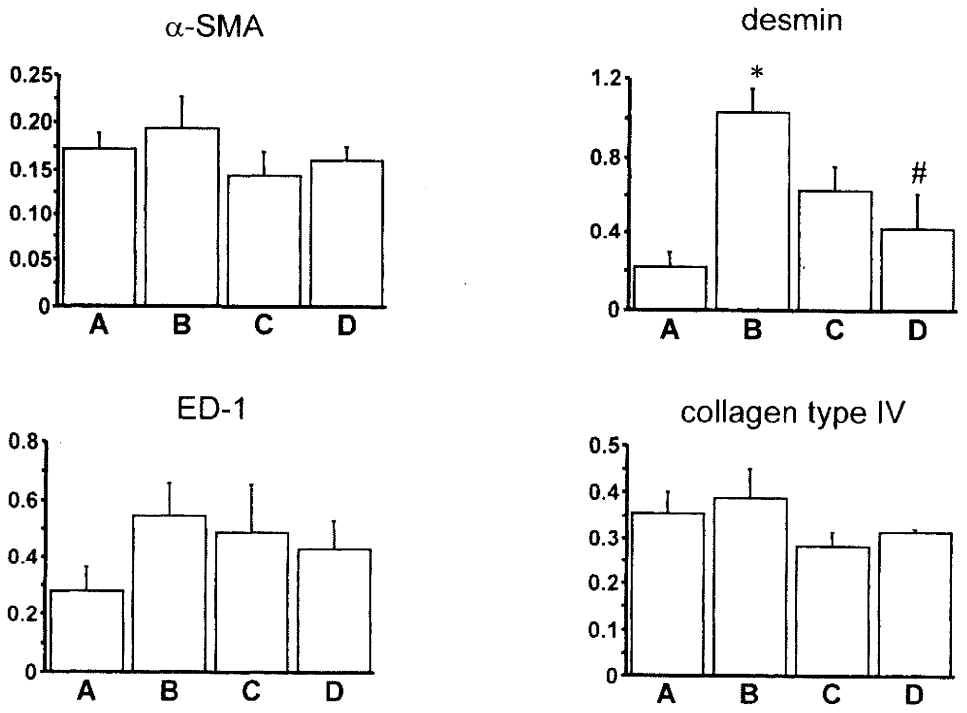

Fig. 4 Immunohistochemical scoring of the glomeruli for α-smooth muscle cell actin (α-SMA), desmin, ED-1, and collagen type IV. A: Wistar rats, B: GK rats treated with vehicle, C: GK rats treated with 2 mg/kg of cyclohexenonic long-chain fatty alcohol (CHLFA), and D: GK rats treated with 8 mg/kg of CHLFA. Data are shown as the means±S.E.M. of three separate determinations in each group. *: Significantly different compared to group A ($P < 0.05$). #: Significantly different compared to group B ($P < 0.05$).

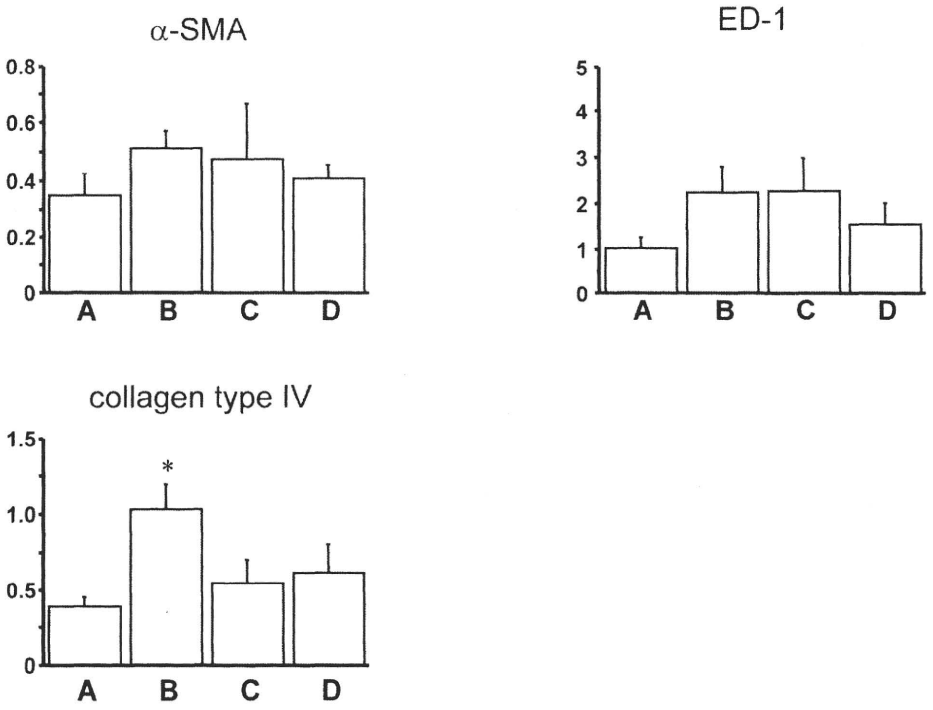

Fig. 5 Immunohistochemical evaluation of renal tubules and peritubular interstitium for α-smooth muscle cell actin (α-SMA), ED-1, and collagen type IV. A: Wistar rats, B: GK rats treated with vehicle, C: GK rats treated with 2 mg/kg of cyclohexenonic long-chain fatty alcohol (CHLFA), and D: GK rats treated with 8 mg/kg of CHLFA. Data are shown as the means± S.E.M. of three separate determinations in each group. *: Significantly different compared to group A ($P < 0.05$).

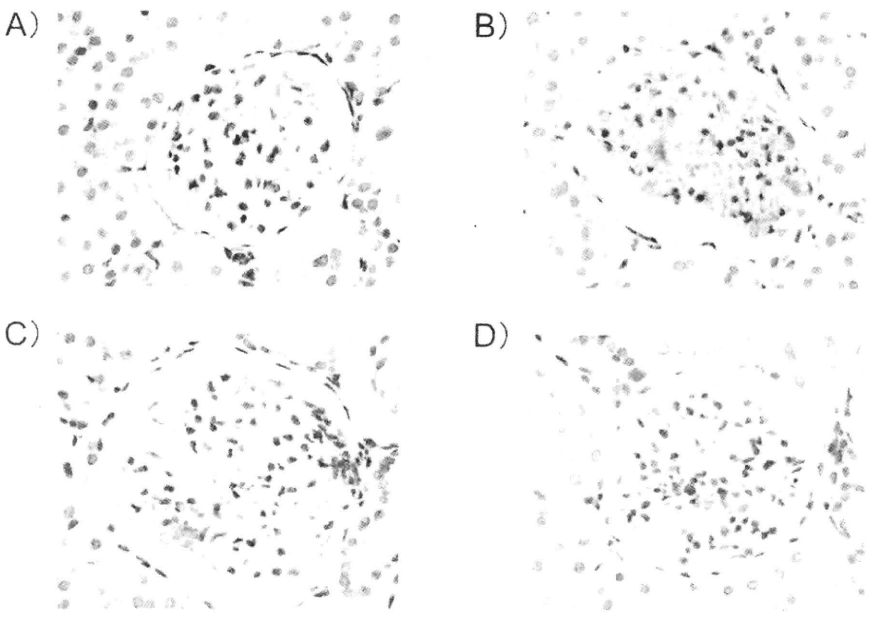

Fig. 6 Immunohistochemical examination of the glomeruli for desmin. A: Wistar rats, B: GK rats treated with vehicle, C: GK rats treated with 2 mg/kg of cyclohexenonic long-chain fatty alcohol (CHLFA), and D: GK rats treated with 8 mg/kg of CHLFA. Desmin expression mostly exhibited an endocapillary pattern and was up-regulated in the untreated GK rat group (B). (×400 magnification)

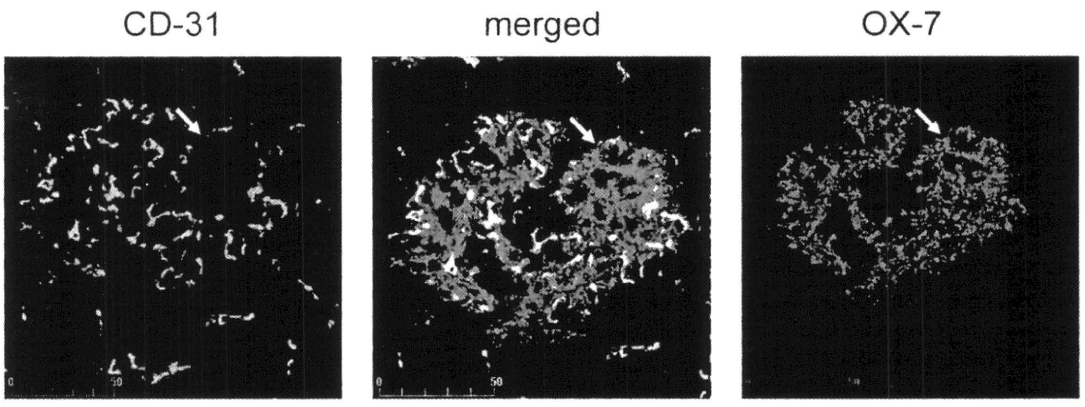

Fig. 7 Immunofluorescent microscopy of the untreated GK rat kidney for CD-31 and OX-7. Nodule-like lesions were observed (arrows).

(Fig. 8f) tended to be more intense than that of control rats (group A) (Fig. 8c), and normal immunostaining intensities were observed in group D (Figs. 8l and 9), although neither result was significant.

DISCUSSION

In this study, we investigated the effects of CHLFA on spontaneous type 2 diabetes-induced nephropathy using a rat model. Treatment with CHLFA did not alter diabetic status—*e.g.*, body weight, urinary excretion, serum glucose, or insulin or blood urea nitrogen levels—but it ameliorated high urinary protein excretion and serum creatinine levels. Treatment with CHLFA also inhibited diabetes-induced increase in kidney weight. CHLFA reduced the glomerular matrix expansion, inhibited the progression of glomerular sclerosis, and improved the glomerular expression of desmin. Our data indicate that CHLFA could prevent type 2 diabetes-induced nephropathy.

The GK rat represents a spontaneous non-insulin-dependent diabetes model. GK rats are produced from normal Wistar rats by repetitive selective breeding, and are widely accepted to be a genetically determined rodent model for human type 2 diabetes. This genetic rat model exhibits a modest degree of renal dysfunctional or structural changes, in addition to the development of glomerular basement membrane (GBM) thickening in animals at 8 to 12 weeks (27). Nobrega and co-workers have also reported that GK rats exhibited a thickening of the GBM, mild mesangial matrix expansion, and glomerular hypertrophy (16). When age-induced progression of glomerular sclerosis was evaluated, glomerular sclerosis of 24-month-old GK rats was more severe than that of 8- or 12-month-old GK rats (23). In type 2 diabetes-induced nephropathy, including that in GK rats, exposure to a prolonged diabetic state occurs.

In the present study, we demonstrated that GK rats exhibited mesangial matrix expansion, segmental glomerular sclerosis, and nodule-like lesions; to our knowledge, few of the previous reports on diabetes-induced nephropathy in GK rats have shown the existence of nodule-like lesions. This discrepancy might be due to differences in the strains of GK rats used or in the durations of the diabetic state. In this study, the nodule-like lesions showed positive staining for OX-7, a mesangial marker, and an absence of staining for PECAM-1, an endothelial marker. These findings indicate that the nodule-like lesions observed here consisted of mesangial matrix. Kimmelstiel-Wilson nodules consist of mesangial matrix and endothelial cells (28), and show positive staining for OX-7 and PECAM-1. Therefore, Kimmelstiel-Wilson nodules differ from the nodule-like lesions observed in the present study, which lacked PECAM-1 expression. In diabetic nephropathy, mesangial extracellular matrix accumulates in the glomeruli, leading to glomerular sclerosis. The overall accumulation of mesangial extracellular matrix is regulated by the relative levels of synthesis and degradation of the matrix, and is determined by a balance between proteases and inhibitors (29). Because CHLFA reduced mesangial matrix expansion, CHLFA may exert its effects on proteases or inhibitors, or both. Further examination of this issue will be necessary in future studies.

Hyperglycemia plays an important role in the development of diabetic nephropathy. Although treatment with CHLFA was not found to alter serum

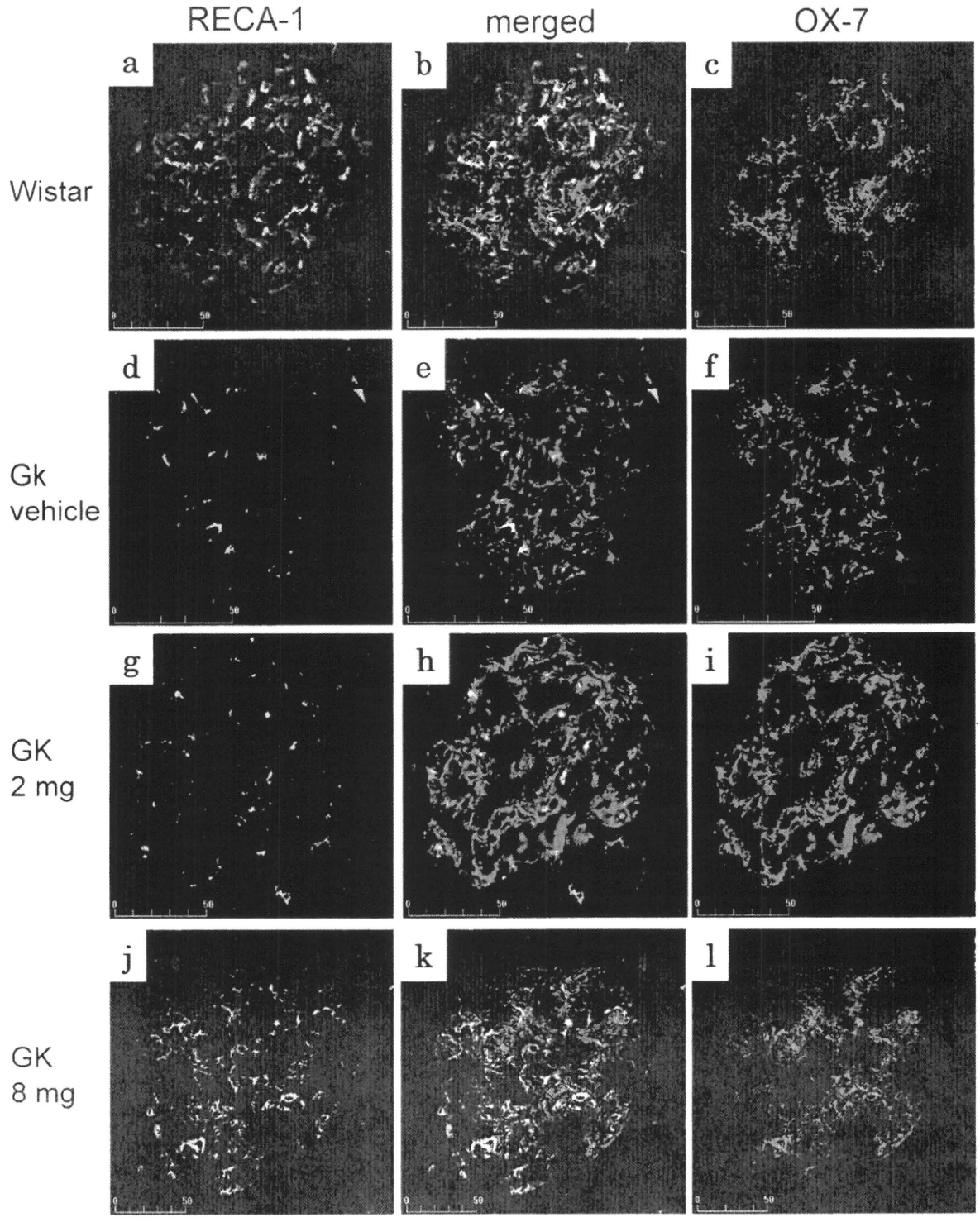

Fig. 8 Immunofluorescent microscopy of the rat kidney for rat endothelial cell antigen-1 (RECA-1) and OX-7. Wistar: Wistar rats (group A), GK vehicle: GK rats treated with vehicle (group B), GK 2 mg: GK rats treated with 2 mg/kg of cyclohexenonic long-chain fatty alcohol (CHLFA) (group C), and GK 8 mg: GK rats treated with 8 mg/kg of CHLFA (group D). The panels **a**, **d**, **g**, and **j** show immunostaining for RECA-1 antibodies. The panels **c**, **f**, **i**, and **l** show immunostaining for OX-7 antibodies. The panels **b**, **e**, **h**, and **k** show merged images.

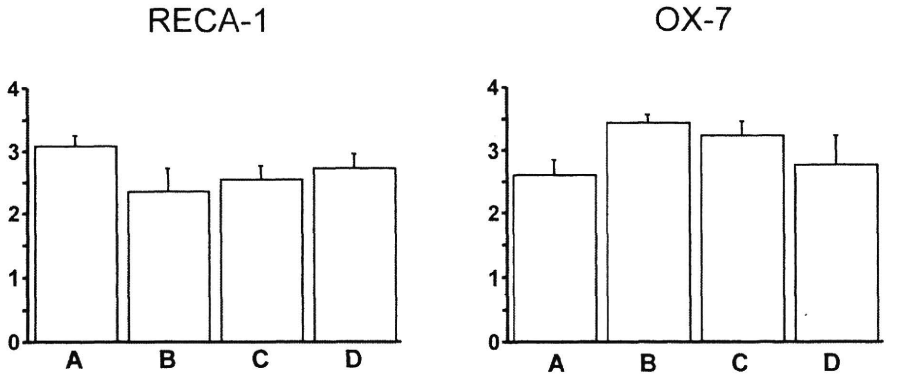

Fig. 9 Immunofluorescent analysis of the kidney for expressions of rat endothelial cell antigen-1 (RECA-1) and OX-7. A: Wistar rats, B: GK rats treated with vehicle, C: GK rats treated with 2 mg/kg of cyclohexenonic long-chain fatty alcohol (CHLFA), and D: GK rats treated with 8 mg/kg of CHLFA. Data are shown as the means ± S.E.M. of five separate determinations in each group.

glucose levels in the present study, it did prevent the progression of diabetic nephropathy similar to that caused by type 1 diabetes (17, 21). It is known that an angiotensin II blockade prevents the progression of diabetic nephropathy without altering glucose levels; CHLFA may exert its effects in a similar manner, although the precise mechanism of such effects, including those at the molecular level, remains unclear at present.

Recently, it has been reported that inhibition of sympathetic nerve activity reduced albuminuria in patients with chronic kidney disease (13), and ameliorated glomerulosclerosis in subtotally nephrectomized rats (1). Another study reported that, by reducing the increased activities of renal sympathetic nerves, the renal efferent arteries could be vasodilated, leading to an improvement in glomerular hypertension (31). It has been reported that CHLFA affects extensions of neurites and differentiations of neurons (2, 3). Watanabe and Miyagawa reported that CFLFA has beneficial effects on peripheral neuropathy and cystopathy in STZ-induced diabetic rats (26). Such effects of CHLFA on neurites and neurons may be one of the mechanisms involved in the alterations of diabetic nephropathy.

The progression of diabetes-induced complications is correlated with endothelial dysfunction, which in turn plays an important role in the progression of diabetic nephropathy (9, 30). Nakagawa and co-workers reported that endothelial NO synthase-knockout mice under diabetic conditions exhibit severe diabetic nephropathy (15). As endothelial cells regulate mesangial cell proliferation (20), diabetes-induced endothelial dysfunction induces mesangial cell injury, in turn leading to mesangial matrix expansion. In this study, high-dose CHLFA treatment was associated with a recovery of capillary density, as shown by immunofluorescence analysis. In our previous reports, we have shown that CHLFA inhibits the progression of diabetes-induced endothelial dysfunction of the aorta in rats with STZ-induced diabetes (10, 25). Here, CHLFA improved diabetes-induced endothelial dysfunction, resulting in the amelioration of diabetic nephropathy.

Podocyte injuries are observed in association with diabetic nephropathy (18), and it is known that injured podocytes express desmin (4, 32). In the present study, diabetic GK rats showed an increased expression of desmin in the glomeruli, and CHLFA reduced this increase. The mechanisms of this effect were not clear, but it is possible that CHLFA exerts direct effects on glomerular podocyte processes, much as it affects neurons (5). It has been reported that the characteristics of podocyte processes closely resemble those of neuronal dendrites. In both podocyte primary processes and neurites, microtubules and intermediate filaments are major cytoskeletal components, and the microtubules contribute to establishment of the mixed polarity in the podocyte primary processes and neurites. Furthermore, the elongation of podocyte processes and neurites is regulated by the same mechanisms as used for membrane transport (11). Therefore, CHLFA may ameliorate diabetes-induced podocyte injury via mechanisms similar to the effects it exerts on neurons, although further investigations will be needed to examine these issues in more detail.

In conclusion, CHLFA was shown to ameliorate type 2 diabetes-induced nephropathy, just as it ameliorates nephropathy caused by type 1 diabetes.

Acknowledgements

This work was published in abstract form at the World Congress of Nephrology (Milan 2009). This study was supported in part by a research grant from the Faculty of Medicine of Tottori University (2008).

REFERENCES

1. Amann K, Rump LC, Simonaviciene A, Oberhauser V, Wessels S, Orth SR, Gross ML, Koch A, Bielenberg GW, Van Kats JP, Ehmke H, Mall G and Ritz E (2000) Effects of low dose sympathetic inhibition on glomerulosclerosis and albuminuria in subtotally nephrectomized rats. *J Am Soc Nephrol* **11**, 1469–1478.
2. Borg J, Toazara J, Hietter H, Henry M, Schmitt G and Luu B (1987) Neurotrophic effect of naturally occurring long-chain fatty alcohols on cultured CNS neurons. *FEBS Lett* **213**, 406–410.
3. Borg J, Kesslak PJ and Cotman CW (1990) Peripheral administration of a long-chain fatty alcohol promotes septal cholinergic neurons survival after fimbria-fornix transection. *Brain Res* **518**, 295–298.
4. Floege J, Alpers CE, Sage EH, Pritzl P, Gordon K, Johnson RJ and Couser WG (1992) Markers of complement-dependent and complement-independent glomerular visceral epithelial cell injury in vivo. Expression of antiadhesive proteins and cytoskeletal changes. *Lab Invest* **67**, 486–497.
5. Gonzalez de Aguilar JL, Girlanda Junges C, Coowar D, Duportail G, Loeffler JP and Luu B (2001) Neurotrophic activity of 2,4,4-trimethyl-3-(15-hydroxypentadecyl)-2-cyclohexen-1-one in cultured central nervous system neurons. *Brain Res* **920**, 65–73.
6. Huang H, Shan J, Pan XH, Wang HP, Qian LB and Xia Q (2007) Carvedilol improved diabetic rat cardiac function depending on antioxidant ability. *Diabetes Res Clin Pract* **75**, 7–13.
7. Janssen U, Riley SG, Vassiliadou A, Floege J and Phillips AO (2003) Hypertension superimposed on type II diabetes in Goto Kakizaki rats induces progressive nephropathy. *Kidney Int* **63**, 2162–2170.
8. Johnson RJ, Iida H, Alpers CE, Majesky MW, Schwartz SM, Pritzi P, Gordon K and Gown AM (1991) Expression of smooth muscle cell phenotype by rat mesangial cells in immune complex nephritis. Alpha-smooth muscle actin is a marker of mesangial cell proliferation. *J Clin Invest* **87**, 847–858.
9. Kanetsuna Y, Takahashi K, Nagata M, Gannon MA, Breyer MD, Harris RC and Takahashi T (2007) Deficiency of endothelial nitric-oxide synthase confers susceptibility to diabetic nephropathy in nephropathy-resistant inbred mice. *Am J Pathol* **170**, 1473–1484.
10. Kazuyama E, Saito M, Kinoshita Y, Satoh I, Dimitriadis F and Satoh K (2009) Endothelial dysfunction in the early- and late-stage type-2 diabetic Goto-Kakizaki rat aorta. *Mol Cell Biochem* **332**, 95–102.
11. Kobayashi N (2002) Mechanism of the process formation: podocytes vs. neurons. *Microsc Res Tech* **57**, 217–223.
12. Koya D, Haneda M, Nakagawa H, Isshiki K, Sato H, Maeda S, Sugimoto T, Yasuda H, Kashiwagi A, Ways DK, King GL and Kikkawa R (2000) Amelioration of accelerated diabetic mesangial expansion by treatment with a PKC beta inhibitor in diabetic db/db mice, a rodent model for type 2 diabetes. *FASEB J* **14**, 439–447.
13. Mena-Martin FJ, Martin-Escudero JC, Simal-Blanco F, Carretero-Ares JL, Arzua-Mouronte D and Castrodeza Sanz JJ (2006) Influence of sympathetic activity on blood pressure and vascular damage evaluated by means of urinary albumin excretion. *J Clin Hypertens (Greenwich)* **8**, 619–624.
14. Murakawa Y, Zhang W, Pierson CR, Brismar T, Ostenson CG, Efendic S and Sima AA (2002) Impaired glucose tolerance and insulinopenia in the GK-rat causes peripheral neuropathy. *Diabetes Metab Res Rev* **18**, 473–483.
15. Nakagawa T, Sato W, Glushakova O, Heinig M, Clarke T, Campbell Thompson M, Yuzawa Y, Atkinson MA, Johnson RJ and Croker B (2007) Diabetic endothelial nitric oxide synthase knockout mice develop advanced diabetic nephropathy. *J Am Soc Nephrol* **18**, 539–550.
16. Nobrega MA, Fleming S, Roman RJ, Shiozawa M, Schlick N, Lazar J and Jacob HJ (2004) Initial characterization of a rat model of diabetic nephropathy. *Diabetes* **53**, 735–742.
17. Okada S, Saito M, Kazuyama E, Hanada T, Kawaba Y, Hayashi A, Satoh K and Kanzaki S (2008) Effects of N-hexacosanol on nitric oxide synthase system in diabetic rat nephropathy. *Mol Cell Biochem* **315**, 169–177.
18. Pagtalunan ME, Miller PL, Jumping-Eagle S, Nelson RG, Myers BD, Rennke HG, Coplon NS, Sun L and Meyer TW (1997) Podocyte loss and progressive glomerular injury in type II diabetes. *J Clin Invest* **99**, 342–348.
19. Raij L, Azar S and Keane W (1984) Mesangial immune injury, hypertension, and progressive glomerular damage in Dahl rats. *Kidney Int* **26**, 137–143.
20. Saeki T, Morioka T, Arakawa M, Shimizu F and Oite T (1991) Modulation of mesangial cell proliferation by endothelial cells in coculture. *Am J Pathol* **139**, 949–957.
21. Saito M, Kinoshita Y, Satoh I, Shinbori C, Kono T, Hanada T, Uemasu J, Suzuki H, Yamada M and Satoh K (2006) N-hexacosanol ameliorates streptozotocin-induced diabetic rat nephropathy. *Eur J Pharmacol* **544**, 132–137.
22. Saito M, Kinoshita Y, Satoh I, Shinbori C, Suzuki H, Yamada M, Watanabe T and Satoh K (2007) Ability of cyclohexenonic long-chain Fatty alcohol to reverse diabetes-induced cystopathy in the rat. *Eur Urol* **51**, 479–488.
23. Sato N, Komatsu K and Kurumatani H (2003) Late onset of diabetic nephropathy in spontaneously diabetic GK rats. *Am J Nephrol* **23**, 334–342.
24. Satoh I, Saito M, Kinoshita Y, Shomori K, Suzuki H, Yamada M, Kono T and Satoh K (2005) Effects of cyclohexenonic long-chain fatty alcohol on diabetic rat trachea. *Life Sci* **77**, 2030–2039.
25. Shinbori C, Saito M, Kinoshita Y, Satoh I, Kono T, Hanada T, Nanba E, Adachi K, Suzuki H, Yamada M and Satoh K (2007) Cyclohexenonic long-chain fatty alcohol has therapeutic effects on diabetes-induced angiopathy in the rat aorta. *Eur J Pharmacol* **567**, 139–144.
26. Watanabe T and Miyagawa I (2002) Effects of long-chain fatty alcohol on peripheral nerve conduction and bladder function in diabetic rats. *Life Sci* **70**, 2215–2224.
27. Yagihashi S, Goto Y, Kakizaki M and Kaseda N (1978) Thickening of glomerular basement membrane in spontaneously diabetic rats. *Diabetologia* **15**, 309–312.
28. Yajima G (1976) A histopathological study on diabetic nephropathy—light and electron microscopic observations. *Acta Pathol Jpn* **26**, 47–62.
29. Zaoui P, Cantin JF, Alimardani-Bessette M, Monier F, Halimi

S, Morel F and Cordonnier D (2000) Role of metalloproteases and inhibitors in the occurrence and progression of diabetic renal lesions. *Diabetes Metab* **26**, 25–29.
30. Zhao HJ, Wang S, Cheng H, Zhang MZ, Takahashi T, Fogo AB, Breyer MD and Harris RC (2006) Endothelial nitric oxide synthase deficiency produces accelerated nephropathy in diabetic mice. *J Am Soc Nephrol* **17**, 2664–2669.
31. Zhou X, Ono H, Ono Y and Frohlich ED (2002) N- and L-type calcium channel antagonist improves glomerular dynamics, reverses severe nephrosclerosis, and inhibits apoptosis and proliferation in an L-NAME/SHR model. *J Hypertens* **20**, 993–1000.
32. Zou J, Yaoita E, Watanabe Y, Yoshida Y, Nameta M, Li H, Qu Z and Yamamoto T (2006) Upregulation of nestin, vimentin, and desmin in rat podocytes in response to injury. *Virchows Arch* **448**, 485–492.

Hepatology Research

Hepatology Research 2010; **40**: 878–886 doi: 10.1111/j.1872-034X.2010.00694.x

Original Article

Epidemiological survey of Japanese children infected with hepatitis B and C viruses

Toshiyuki Iitsuka, Jun Murakami, Ikuo Nagata, Susumu Kanzaki and Kazuo Shiraki

Division of Pediatrics and Perinatology, Faculty of Medicine, Tottori University, Yonago, Japan

Aim: The lack of a nationwide survey on hepatitis B virus (HBV) and hepatitis C virus (HCV) infections in Japan led us to investigate the epidemiological profiles of these infections among Japanese children.

Methods: We conducted a questionnaire survey of children (<20 years of age) infected with either HBV ($n = 136$) or HCV ($n = 114$), who visited 636 pediatric institutions in Japan from 2003 through 2005. Most HBV-infected subjects (94%) were born in 1986 or after when a nationwide immunization program for infants born to HBe antigen-positive carriers was initiated. The transmission routes were divided into five groups: maternal, horizontal (subdivided into intrafamilial, iatrogenic and other horizontal), and unknown transmission.

Results: Comparison of subjects born in 1990 or after and those born in 1989 or before, when anti-HBc and anti-HCV (c100-3) screening tests of blood donors began, showed a shift in the relative proportions of maternal, intrafamilial, iatrogenic, other horizontal, and unknown transmission from 52%, 19%, 4%, 7% and 19% to 70%, 14%, 6%, 1% and 9%, respectively, for HBV, which was statistically insignificant ($P = 0.120$), and from 14%, 0%, 76%, 4% and 7% to 89%, 2%, 4%, 0% and 5%, respectively, for HCV, which was statistically significant ($P < 0.001$). HBV horizontal transmission did not decrease in proportion. No transfusion-acquired HCV infection was reported in subjects born in 1993 or after.

Conclusion: Maternal transmission is a prominent source of HCV infection among Japanese children. The implementation of measures to prevent HBV horizontal infection is also essential, and the present system of selective vaccination should be expanded to universal vaccination.

Key words: children, hepatitis B virus, hepatitis C virus, transmission route

INTRODUCTION

THE MAJOR TRANSMISSION routes of hepatitis B virus (HBV) and hepatitis C virus (HCV), which are representative agents of blood-borne infections causing hepatitis, are maternal transmission, blood transfusion, intrafamilial contact, sexual intercourse and i.v. drug use. Improvements in the screening of blood donors have led to a rapid decrease in blood transfusion-related infections of both viruses.[1,2] Regarding preventive measures against these infections by other routes, immunoprophylaxis by vaccine is available for HBV, but not for HCV.

In Japan, passive and active immunoprophylaxis of babies born to carrier mothers with hepatitis B surface antigen (HBsAg) and hepatitis B e antigen (HBeAg) by combined hepatitis B immunoglobulin (Ig) and vaccine has been performed since 1986 using a selective vaccination policy. This policy was successful in terms of reducing the number of HBV carrier infants contracting the virus from their HBV carrier mothers.[3–6] Following the establishment of this vaccine program, the annual rate of HBV carriers was estimated to decrease from 0.26% of all babies in 1985 to 0.04% in 1992 and 0.024% in 1995.[7] Since 1995, this program was extended to carrier mothers with HBsAg regardless of the mother's HBeAg/anti-HBe antibody (anti-HBe) status. However, a universal vaccination program for all children has not been established yet. As a result, most Japanese young adults are therefore considered to remain susceptible to HBV.[5,8]

Under these circumstances, the occurrence of adult acute HBV infection is currently showing an increasing tendency in Japan. It tends to occur mostly in young men, and genotype A, which was imported from overseas and is mainly transmitted by sexual contact with

Correspondence: Dr Toshiyuki Iitsuka, Division of Pediatrics and Perinatology, Faculty of Medicine, Tottori University, 36-1 Nishi-cho, Yonago, Tottori 683-8504, Japan. Email: tiitsuka-ttr@umin.ac.jp
Received 3 March 2010; revision 22 May 2010; accepted 25 May 2010.

multiple partners, shows an increasing proportion.[9–13] Because HBV genotype A has a relatively high tendency to become chronic, adult chronic infection is expected to increase in the future. As a result, there is concern regarding the occurrence of hepatitis B among children, which should also be investigated.

Concerning HCV, the prevalence rate of anti-HCV antibody (anti-HCV) among Japanese blood donors has decreased yearly depending on the year of birth,[14] and there have been no reports of an increasing tendency in HCV infection among adults or children in Japan. In Italian children, HCV infection is mainly caused by maternal transmission,[15] and it is expected to decrease because HCV shows low efficiency of vertical and household transmission, which are responsible for the spread of childhood hepatitis B in endemic areas, and also because children and adolescents have limited exposure to highly efficient routes of transmission such as parenteral drug abuse.[16] It is therefore expected that similar observations will also be made in Japan.

A national survey on HBV and HCV carriers has not been conducted yet, making it difficult to accurately assess the epidemiological features. The transmission rates by the different infection routes appear to differ between HBV and HCV, but the risk factors for virus acquisition are considered to be similar between them since both are blood-borne viruses. Therefore, investigating HBV and HCV infections together will help to establish effective new management strategies to eliminate these two infections.

Instead of a national surveillance program, the aim of this study is to carry out a questionnaire survey on children with HBV and HCV infections throughout the country, to investigate the incidence, routes of transmission and clinical pictures of these diseases, and to consider the management and preventable measures after implementation of the current blood donor screening tests and national HBV vaccination programs for high-risk infants born to HBV carrier mothers in Japan.

METHODS

Questionnaire

A QUESTIONNAIRE SURVEY was conducted in 2007 at a total of 636 institutions, including pediatric departments of university hospitals, departments of internal medicine at children's hospitals, and pediatric departments of general hospitals with at least 300 beds in Japan. Institutions of internal medicine were excluded but those of transplant surgery were included.

The subjects of this questionnaire were children under 20 years of age, who were infected with either HBV or HCV and had visited any of the relevant institutions in the 3 years from January 2003 to December 2005. Therefore, it is a survey of patients who visited for the first time during this period, as well as those who had visited for the first time in 2002 or before, and visited again during 2003–2005. Patients with either HBsAg or HBV DNA positive were diagnosed with HBV infection, and those with either HCV core antigen or HCV RNA positive were diagnosed with HCV infection.

The anonymous questionnaire form included the patient's background data such as date of birth, sex, age at the time of the first hospital visit and age at the time of the diagnosis, as well as the laboratory findings supporting the diagnosis. The presumed transmission routes were also reported according to the following categories: (i) maternal transmission including vertical transmission and horizontal transmission from mother to child; (ii) intrafamilial transmission other than maternal transmission including transmission from the father, grandparents or siblings; (iii) iatrogenic transmission including blood transfusion and transplantation; (iv) other horizontal transmission including sexual intercourse and i.v. drug use; and (v) unknown transmission. Other transmission than maternal (excluding unknown transmission) was therefore described as horizontal. As for children infected with HBV by maternal transmission, a history of hepatitis B Ig (HBIG) administration and HB vaccination was also clarified as far as possible. Investigated hepatitis virus markers included HBsAg, anti-HBs antibody (anti-HBs), HBeAg, anti-HBe and HBV DNA for cases of HBV infection and anti-HCV, HCV RNA and HCV core antigen for cases of HCV infection.

The clinical conditions were categorized as follows: constantly normal transaminase levels, occasionally abnormal transaminase levels, chronic hepatitis, cirrhosis, hepatocarcinoma, acute hepatitis and fulminant hepatitis in case of HBV infection, and constantly normal transaminase levels, occasionally abnormal transaminase levels, continuously abnormal transaminase levels for at least 6 months, cirrhosis and hepatocarcinoma in case of HCV infection.

Patients

The questionnaire was sent by mail to 636 institutions, and a response was received from 268 institutions (response rate 42%). We extracted a total of 164 HBV-infected children meeting the inclusion criteria of our